Energy Dependence of Proton-Induced Xenon Fragmentation and the Approach to Liquid-Gas Criticality in Nuclear Matter

M. Mahi, A. T. Bujak, D. D. Carmony, Y. H. Chung,[a] L. J. Gutay, A. S. Hirsch, G. L. Paderewski,[b] N. T. Porile, T. C. Sangster,[c] R. P. Scharenberg, and B. C. Stringfellow

Department of Physics and Department of Chemistry, Purdue University, West Lafayette, Indiana 47907

(Received 29 May 1987)

Cross sections ascribed to a multifragmentation process have been obtained from the measured fragment yields ($3 \leq Z_f \leq 14$) in proton-xenon interactions ($1 \leq E_p \leq 20$ GeV). The variation of the yields with both mass and bombarding energy can be understood by use of the droplet model of the liquid-gas phase transition. With increasing energy, this model indicates that multifragmentation occurs first in the mechanical-instability region, next in the supersaturated vapor, and finally in the critical region.

PACS numbers: 25.40.Sc, 21.65.+f

We have recently studied the inclusive production of light fragments ($3 \leq Z_f \leq 14$) in the interaction of xenon with 1–20-GeV protons. The experiment was performed at the Brookhaven Alternating Gradient Synchrotron (AGS) utilizing an internal-gas-jet target and gas-ΔE-solid-state-E detectors to study fragment production at 48.5° and 131.5° to the beam over a nearly continuous range of proton energies in the above interval. In a recent Letter,[1] we fitted the fragment kinetic-energy spectra with an expression based on the droplet model of multifragmentation.[2] Excellent fits to the data were obtained for proton energies of 9 GeV and higher with essentially the same parameters used to fit similar data previously obtained by us at Fermilab energies.[2-6] However, below 6 GeV, we found evidence for an additional component in the spectra, which increased in relative magnitude with decreasing proton energy. We attributed this second component to a binary breakup process, a mechanism that can be understood as part of the continuum of statistical breakup processes ranging from evaporation to binary fission.[7] We were able to decompose the steeply increasing cross sections for fragment production observed up to $\simeq 10$ GeV into essentially constant cross sections for binary fragment production and even more steeply increasing cross sections above a predicted threshold in the vicinity of 1 GeV for multifragmentation.[8]

In the present report we apply the droplet model to the high-energy component and show that the evolution of the fragment yields with mass and bombarding energy can be understood in the context of the liquid-gas phase transition. The experimental procedure has been described elsewhere.[1,9]

The description of a gas of noninteracting clusters in thermal equilibrium has been given by Fisher in his droplet model.[10] The number of clusters per unit volume containing n constituents depends on the Helmholtz free energy of the cluster f_n, the chemical potential per particle μ, and the temperature T, as

$$\rho_n = \rho_0 n^{-\tau} \exp[-(f_n - \mu n)\beta], \quad (1)$$

where $\beta = 1/k_B T$. The free energy contains contributions from both the volume and surface free energy of the droplets. Separating the bulk and surface terms, we can write Eq. (1) as[10]

$$\rho_n = \rho_0 n^{-\tau} X^{n^\sigma} Y^n. \quad (2)$$

The factor X arises from the surface free energy of the droplet; Y contains the volume free energy and the chemical potential. The critical point, $T = T_c$, $\rho - \rho_c$, occurs when $X = Y = 1$. Below the critical point, $X < 1$ and $Y > 0$. The liquid-gas coexistence curve corresponds to $Y = 1$; when $Y > 1$ the vapor is supersaturated. The temperature dependence in Eq. (2) is contained in X and Y. The parameter ρ_0 gives an overall normalization; τ and σ are critical exponents.

We have fitted our data with Eq. (2), assuming that the cross section for the production of a fragment is proportional to the number of fragments of a given nucleon number per unit volume. Although we did not measure the nucleon number of each fragment, but instead its charge, we have used the data acquired in the limiting fragmentation region[2] to find an average nucleon number $\langle A_f \rangle$ for a given Z_f. This value of A_f served as the number of nucleons [n in Eq. (2)] in a fragment of a given Z_f. For each of the eleven E_p bins there corresponds a value of X and a value of Y determined from the fit. A single value of the overall normalization factor was used. In addition, τ was fixed at 2.2 and σ at 0.6386, the experimental values for a liquid-gas phase transition.[11] For each of the data sets, forward and backward, ten data points were fitted with the two adjustable parameters, X and Y. The results of the two sets differ only in the value of the overall normalization constant. Therefore, in what follows, we will concentrate on the forward-angle data.

The comparison between the fit and the data can be viewed in two ways, i.e., σ vs E_p at a given A, or σ vs A at a given E_p. Figure 1 shows some typical excitation functions. It is clear that the fitted curves reproduce the general trends of the data. The sharply increasing excitation functions up to $\simeq 10$ GeV reflect the increase with

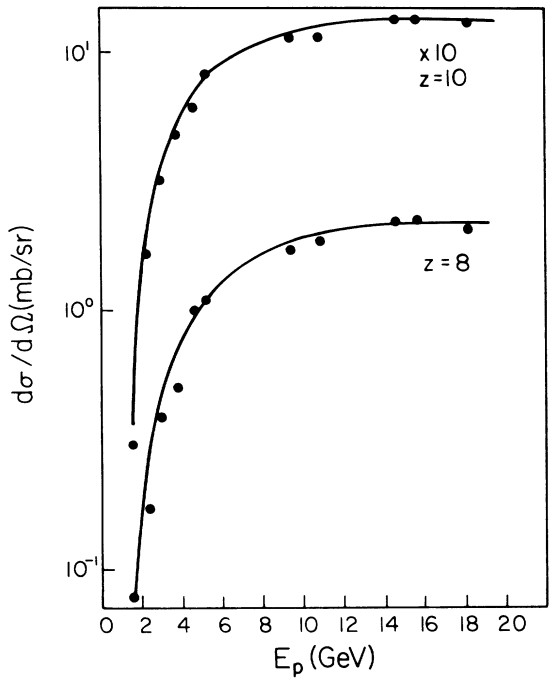

FIG. 1. Excitation functions of O and Ne fragments emitted at 48.5° to the beam. Circles are experimental, with binary component subtracted. Curves: Fit of Eq. (2).

proton energy in the excitation energy deposited in the central collisions that result in multifragmentation.[12] In turn, the increasing excitation energy largely reflects the increase in the number of collisions, primarily inelastic, made by the incident proton in a central collision, and in the energy loss per collision.[13]

Figure 2 shows the variation of $d\sigma/d\Omega$ with A_f for two typical E_p bins. It is remarkable that the droplet model can fit both the mass and energy dependence of the fragment yields. To be sure, there are some systematic deviations from the curve in Fig. 2. For example, the data point corresponding to carbon lies above the fitted curve for all eleven bins. However, it must be remembered that Eq. (2) assumes a slowly varying binding energy per particle as a function of constituent number and a single type of constituent particle.[10]

The values of X and Y obtained from the fitting procedure are shown as functions of E_p in Fig. 3. The errors in X and Y were estimated by use of the Monte Carlo method. Starting from the measured fragment cross sections, we generated new data sets assuming a Gaussian distribution having a mean equal to the measured cross section and a standard deviation equal to the error in the cross section ($\simeq$10%). Values of X and Y were then determined for each new data set and their standard deviation was found to be 1%. It is seen that both X and Y approach unity above 10 GeV, where fragment production enters the limiting fragmentation region. This result is independent of the overall normalization.

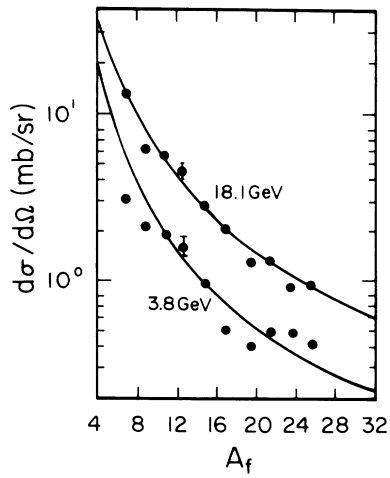

FIG. 2. Mass dependence of fragment cross sections for the indicated E_p.

Within the context of the droplet model, we can conclude that the temperature of the fragmenting system increases with E_p and approaches the critical value at $\simeq$10 GeV. Comparing Fig. 3 to Fig. 1, one can further see that the increase in $d\sigma/d\Omega$ parallels that in the parameter X. Thus, according to the model, the increase in X accounts for the increasing fragment production cross sections.

Although the droplet formula (2) was derived in the thermodynamic limit of infinite particle number, we have applied it to a case in which $n\simeq100$. As such, it is not strictly correct to speak of a sharp phase transition.[14] The effects of finite particle number on T_c have been explored for $N=Z$ systems with no Coulomb force. For a system of 100 particles, $T_c(100)\simeq0.75T_c(\infty)$.[15] The Coulomb force is predicted to be responsible for a further reduction of a few megaelectronvolts.[15]

Our analysis indicates that the liquid-gas critical region may be reached at a proton energy above 10 GeV. How are fragments produced at lower energies? Figure

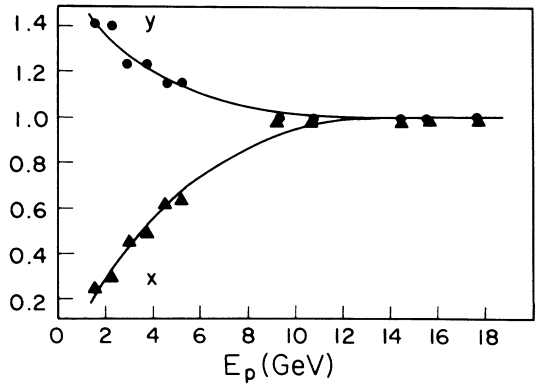

FIG. 3. The parameters X and Y obtained from fit of Eq. (2).

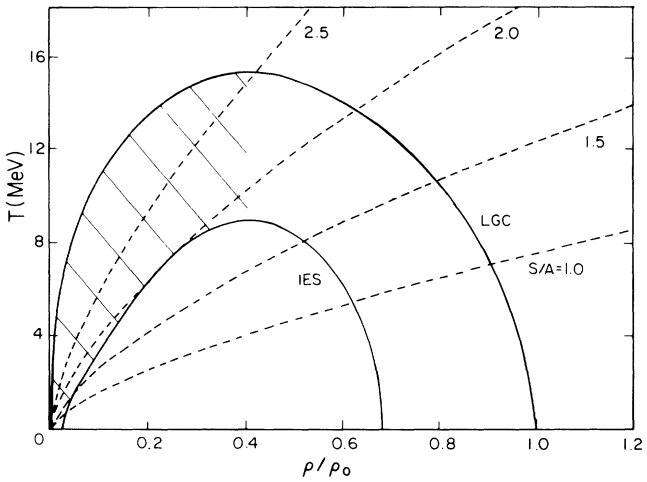

FIG. 4. Phase diagram of nuclear matter. LGC: liquid-gas coexistence curve; IES: isentropic spinodal. The dashed curves represent isentropic trajectories for the indicated values of S/A. The hatched area is the metastable region of supersaturated vapor.

4 shows a phase diagram of nuclear matter obtained with an equation of state derived from a zero-range Skyrme-type interaction.[16] Let us examine our results in terms of this diagram on the assumption that reaction trajectories leading to fragmentation follow the isentropic expansions shown by the dashed lines.[16,17] To do so we must estimate the entropy generated in interactions leading to fragment production as a function of E_p. Nakai *et al.*[18] have shown that central collisions of 1–4-GeV protons with nuclear targets lead to the forward emission of a moving source of nucleons and pions, which on average carries away some 75% of the incident kinetic energy. The remaining 25% of the energy is deposited as excitation energy in the residual nucleus, which is substantially reduced in nucleon number. Thus, we estimate that the remnant of a 4-GeV p-Xe central collision ($A_r \simeq 100$) has an excitation energy E^* of about 1 GeV.

An independent estimate of this value can be obtained from a recent simulation of central collisions,[19] which showed that the multifragment mass yield distribution for a given E_p can be parametrized as

$$\text{Yield}\ (A_f) \propto A_f^{-\tau'}. \tag{3}$$

Comparison with Eq. (2) shows that the temperature dependence of X and Y has been incorporated in the value of an effective power-law exponent τ'. It is argued[19] that a plot of τ' vs E_p should go through a minimum at an energy for which the average E^* is equal to the total binding energy of the nucleus, i.e., $\simeq 0.9$ GeV for the remnant of a p-Xe interaction. We have fitted Eq. (3) to our data and show the variation of τ' with E_p in Fig. 5. The error in τ' was estimated in the manner described above for X and Y and was found to be 4%. A minimum is observed at $E_p \simeq 4$ GeV, and τ'

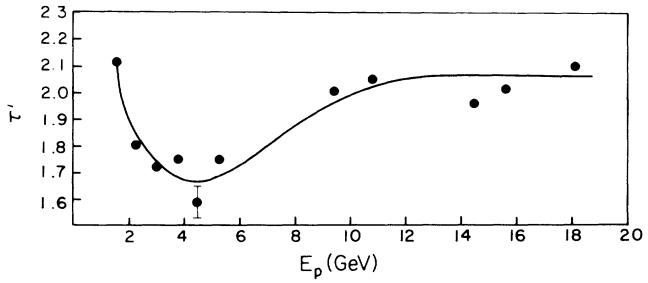

FIG. 5. Dependence of τ' on E_p. The curve is drawn to guide the eye.

levels off at $\simeq 2.1$ at high energies.[20] We conclude that at 4 GeV $E^* \simeq 0.9$ GeV, in agreement with the value derived from Nakai *et al.*[18]

The agreement between these two independent estimates of E^* encourages us to use the Nakai estimates of this quantity for $E_p = 1$–4 GeV. Values of initial T and S/A can be derived from E^* on the basis of the Fermi-gas model: $E^* = A_r T_i^2/10$ and $S/A = T_i/5$. At the lowest E_p measured, 1.6 GeV, $T_i \simeq 6$ MeV and $S/A \simeq 1$. Figure 4 shows that at these low entropies the isentropic spinodal is reached and fragmentation can occur in the mechanical-instability region.[17] However, the fragment production cross sections are only $\simeq \frac{1}{10}$ of their limiting value indicating that this process is not very probable. The estimated value of T_i compares favorably with experimental[21] and calculated[22] values of the temperature at which the binary breakup of a compoundlike nucleus gives way to multifragmentation. Our observation[1] of a transition in the fragment production mechanism at these low energies also is in accord with these temperature estimates.

At $E_p \simeq 4$ GeV, we estimate $S/A \simeq 2$. Figure 4 shows that a reaction trajectory with this S/A value can reach the metastable phase of supersaturated vapor. Fragment formation then corresponds to droplet formation in a supersaturated vapor ($Y > 1$).[14]

The change in T and S/A as the beam energy increases from 4 GeV to the limiting fragmentation region can be estimated as follows. The parameter X is related to the surface properties of a drop at temperature T by[14]

$$-\ln(X) = (18/T)(1 + \tfrac{3}{2}\, T/T_c)(1 - T/T_c)^{3/2}. \tag{4}$$

At $E_p = 4$ GeV the value of X is approximately 0.53. In the limiting fragmentation region $X \simeq 1$. A choice of T_c in the 12–16-MeV range leads to increases in T and S/A of some 30%. Thus we estimate $S/A \simeq 2.6$ when $E_p > 10$ GeV. Figure 4 shows that a trajectory with S/A of this magnitude reaches the critical region. Thus, entropy estimates in conjunction with the phase diagram support the conclusion based on the limiting values of X and Y.

In summary, we have described the threshold behavior of fragment production cross sections using the droplet-model parametrization. Multifragmentation is a high-

energy phenomenon involving excitation energies comparable to the total binding energy of the nucleus. Cross sections for multifragment production become appreciable when the entropy generated in the target is a significant fraction of the limiting entropy for a system of finite particle number. Our analysis in terms of the liquid-gas phase transition is consistent with the following picture: With increasing bombarding energy, multifragmentation occurs first in the mechanical instability region, then in the supersaturated vapor, and, finally, at limiting energies ($E_p > 10$ GeV), in the critical region. The fragment production cross sections show a concomitant order-of-magnitude increase. We find it remarkable that the critical region should be reached at the energy where the cross sections attain their asymptotic values. It would be of interest to determine whether this effect is unique to targets in the xenon mass region or whether it reflects a more general behavior.

We would like to thank the members of the Alternating Gradient Synchrotron (AGS) Division at Brookhaven National Laboratory and express our gratitude to A. Pendzick, J. Tuozzolo, H. Hseuh, R. Skelton, J. Glenn, M. Zguris, H. Foelsche, and especially to K. Reece and the other operators in the AGS main control room for their assistance during the jet target facility installation and operation. We acknowledge useful discussions with Y. E. Kim, P. F. Muzikar, and H. Nakanishi. This work was supported by the U.S. Department of Energy. This work was submitted by one of us (M.H.) in partial fulfillment of the requirements for the Ph.D degree.

[a]Present address: Department of Chemistry, Hayllym University, 1 Okchun-Dong, Chooncheon 200, Korea.

[b]Present address: Mission Research Corporation, 4935 N. 35th St., Colorado Springs, CO 80919.

[c]Present address: Lawrence Livermore National Laboratory, P. O. Box 808, MS 1-208, Livermore, CA 94550.

[1]T. C. Sangster *et al.*, Phys. Lett. B **188**, 29 (1987).

[2]A. S. Hirsch *et al.*, Phys. Rev. C **29**, 508 (1984).

[3]J. E. Finn *et al.*, Phys. Rev. Lett. **49**, 1321 (1982).

[4]R. W. Minich *et al.*, Phys. Lett. B **118**, 458 (1982).

[5]A. S. Hirsch *et al.*, Nucl. Phys. **A418**, 267c (1984).

[6]N. T. Porile *et al.*, Phys. Lett. **156B**, 177 (1985).

[7]L. Moretto, Nucl. Phys. **A247**, 211 (1975).

[8]D. H. E. Gross *et al.*, Phys. Rev. Lett. **56**, 1544 (1986).

[9]B. C. Stringfellow *et al.*, Nucl. Instrum. Methods A **251**, 242 (1986).

[10]M. E. Fisher, Physics (N.Y.) **3**, 255 (1967), and Rep. Prog. Phys. **30**, 615 (1967).

[11]J. C. LeGuillon and J. Zinn-Justin, Phys. Rev. B **21**, 3976 (1980).

[12]A. I. Warwick *et al.*, Phys. Rev. C **27**, 1083 (1983).

[13]J. Cugnon, Nucl. Phys. **A462**, 751 (1987).

[14]A. L. Goodman *et al.*, Phys. Rev. C **30**, 851 (1984).

[15]H. R. Jaqaman *et al.*, Phys. Rev. C **29**, 2067 (1984).

[16]D. H. Boal and A. L. Goodman, Phys. Rev. C **33**, 1690 (1986).

[17]J. A. Lopez and P. J. Siemens, Nucl. Phys. **A431**, 728 (1984).

[18]K. Nakai *et al.*, Phys. Lett. **121B**, 373 (1983).

[19]T. J. Schlagel and V. R. Pandharipande, Phys. Rev. C **36**, 162 (1987).

[20]When the data of our Fermilab experiment (Ref. 2) for the identical mass range are reanalyzed by means of Eq. (3) with an average mass number at each Z to replace the actual mass-yield distribution, the value of τ' decreases from 2.6 to 2.3. The remaining discrepancy between this value and $\tau' \simeq 2.1$ observed at 12–19-GeV may be the result of the large difference between AGS and Fermilab energies and of the difference in the angles at which fragment emission was detected in the two experiments.

[21]S. Song *et al.*, Phys. Lett. **130B**, 14 (1983).

[22]J. P. Bondorf *et al.*, Nucl. Phys. **A444**, 460 (1985).